Initial Adhesion Characteristics of Polymer Modified Binder

Transfund New Zealand Research Report No.178

Initial Adhesion Characteristics of Polymer Modified Binders

M.C. Forbes
P.R. Herrington
J.E. Patrick
Opus Central Laboratories
Lower Hutt, New Zealand

Transfund New Zealand Research Report No. 178

ISBN 0-478-11589-X
ISSN 1174-0574

P O Box 2331, Lambton Quay, Wellington New Zealand
Telephone 64-4-473-0220; Facsimile 64-4-499-0733

M. C. Forbes, P. R. Herrington, J. E. Patrick 2000. Initial Adhesion Characteristics of Polymer Modified Binders. *Transfund New Zealand Research Report 178.* 35 pp.

Keywords: adhesion, aggregate, bitumen, chipseals, polymer modified binders, roads, wetting.

An Important Note for the Reader

The research detailed in this report was commissioned by Transfund New Zealand.

Transfund New Zealand is a Crown entity established under the Transit New Zealand Act 1989. Its principal objective is to allocate resources to achieve a safe and efficient roading system. Each year, Transfund New Zealand invests a portion of its funds on research that contributes to its objective.

While this report is believed to be correct at the time of its preparation, Transfund New Zealand, and its employees and agents involved in preparation and publication, cannot accept any liability for its content or for any consequences arising from its use. People using the contents of the document should apply, and rely upon, their own skill and judgement. They should not rely on its contents in isolation from other sources of advice and information.

The report is only made available on the basis that all users of it, whether direct or indirect, must take appropriate legal or other expert advice in relation to their own circumstances. They must rely solely on their own judgement and seek their own legal or other expert advice in relation to the use of this report.

The material contained in this report is the output of research and should not be construed in any way as policy adopted by Transfund New Zealand but may form the basis of future policy.

Contents

Executive Summary

Polymer modified binders (PMBs) are increasingly being used in New Zealand roads to cope with the larger stresses imposed by increasing traffic volumes. However the addition of a polymer to a binder may change the conditions required to achieve good initial wetting and adhesion of the binder onto the aggregate. This project intended to measure: how quickly the PMB spreads across and wets an aggregate surface, the adhesion strength between the binder and aggregate, and how well it resists water stripping.

It has been well established in the research literature that adhesion between a fluid and a solid surface can change the rheology of many fluids, and in particular some bituminous binders. This change occurs in a thin layer near the solid surface, generally increasing the viscosity from that of the bulk of the fluid. The intention in this project was to use different aggregate materials as the parallel plate surfaces in a Dynamic Shear Rheometer (DSR) to measure this effect. However during the trial phase of the project this could not be detected at a level above the normal measurement uncertainties. This may have been due to the particular PMB/aggregate combination used not having a stronger adhesive layer, or that layer being thinner than expected (which would require measurements with even narrower gaps between the DSR plates). Thus further work would be required to see if this measuring technique could be developed into a test to measure adhesion.

An attempt was made to measure early adhesion failure via the effect on the apparent shear modulus as injected water lifts the PMB away from the bottom plate of the DSR (water stripping). For the case of a stainless steel 'aggregate', the water tunnelled through the middle of the PMB rather than the aggregate/PMB interface, implying the adhesion was stronger than the PMB's cohesion. With the greywacke aggregate, no change in modulus was detected although the water was clearly flowing out of the system. Inspection of the samples after the experiment found no sign of the water in the PMB, suggesting the water was flowing through the greywacke itself.

The final part of the project involved measuring the rate at which a drop of binder spreads across an aggregate surface. Aggregates have a large variability in the rock making up any particular surface which may cause problems for the repeatability of the measurements. For this reason sandpaper was used instead to provide the 'aggregate' surface, while real aggregate surfaces could be measured in later work. Various combinations of binder type (of base bitumen and polymer concentration), drop size, and sandpaper grade (giving different surface textures) were measured at selected temperatures. A simple power law gives a reasonable description of the spreading rates, which show the expected dependence on viscosity and drop size. However some (second order) discrepancies were found, possibly due to elastic oscillations or steric hardening of the binder, which need further investigation. The largest influence on the spreading rates is temperature, for instance a 3%SBS130 binder takes ten times longer to cover the same area when the temperature drops from 40 °C to 30 °C. The spreading rates were also found to depend on the surface roughness, which is not accounted for in current theory. Measurements at 40 °C were found to give good discrimination between binders with acceptable/unacceptable spreading rates, but this finding needs to be calibrated against field results before the method could be put forward for consideration as a standard test.

Abstract

This report describes work to investigate sealing aggregate bonding to standard and polymer modified bituminous binders. The work included investigation of the variation of adhesion strength for different aggregate surfaces, the effect of water on binder-aggregate bonding, and development of a test for measuring binder spreading rate on plane surfaces. The spreading rate test was generalised to rough surfaces, and results fitted to power law equations for degree of spreading. This test has the potential to become a standard method for evaluating aggregate-binder adhesion, but further work with various aggregate surfaces and comparison with field-trial results is needed to achieve this.

1. Introduction

Polymer modified binders (PMBs) are being increasingly used in New Zealand roads to cope with the larger stresses imposed by the heavier trucks and greater traffic volumes of recent years. However, the changes in mechanical properties brought about by the addition of a polymer to a binder, while generally believed to be desirable for long term performance, also change the conditions required to achieve good initial wetting and adhesion of the binder onto the chip. In particular, the highly elastic nature of styrene-butadiene-styrene (SBS) modified bitumens is recognised by practitioners as presenting special problems in routinely obtaining good initial chip adhesion.

Bitumen/chip adhesion is known to depend on a combination of chemical and mechanical interactions. The chemical attraction/adsorption of binder components to the aggregate is unlikely to be altered by the addition of polymers. However, the mechanical interaction of the binder and aggregate surface is highly dependent on the physical properties of the binder. The way in which the binder flows over the aggregate surface and into the micro-texture will depend on both the absolute magnitude of the modulus and relative size of the viscous and elastic components. The object of this research is to obtain useful quantitative information on the relationship between these properties and chip wetting and adhesion.

2. Effect of Aggregate Surface on Adhesion

The existence of slip (due to lack of adhesion) between a liquid and the surfaces of rheometer plates is a well known 'problem' in rheology. The other side of the coin is that adhesion between the sample and rheometer plates may alter the properties being measured. Indeed, there have been many studies showing at the bitumen/aggregate interface a thin layer may form with different rheological properties from that of the bulk bitumen (Mack (1957), Bikerman (1966), Ensley (1975), Gastmans (1996)). Fink and Griffin (1961) find films thinner than ~20 μm have their viscosity affected by the choice of aggregate surface used in a sliding plate viscometer. Ensley and Scholz (1972) measured the heat generated from the energy of adhesion when aggregate is immersed in bitumen. Scholz and Brown (1996) modify a Dynamic Shear Rheometer and find some bitumen's are affected by the aggregate type, but require a statistical analysis (ANOVA) to detect these (small) differences. Huang, Robertson, McKay, and Branthaver (1998) use a sliding plate viscometer and find thin films (< 50 μm) for some bitumen/aggregate combinations have different viscosities than thick films, especially at low shear rates.

The intention in this project was to measure the effect the aggregate/bitumen adhesion layer has on the complex shear modulus (G^*) using a dynamic shear rheometer. Sets of rheometer plates with different aggregates glued to them were to be used in addition to the normal stainless steel (control) plates. To allow for variations between different samples of the same bitumen (and to fit equation (1), discussed below), each sample is to be first measured at a large gap (e.g. 1 mm) and then progressively squashed down to a smaller gaps and re-measured.

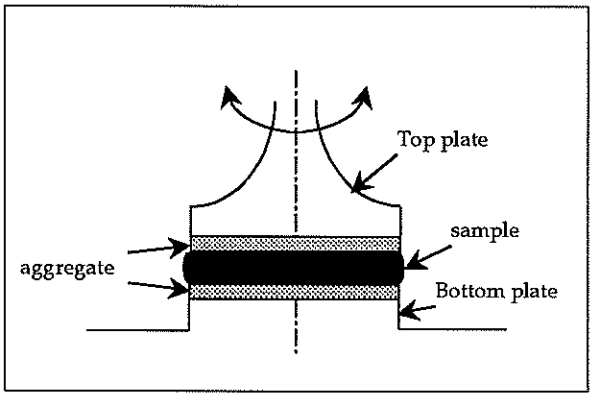

The sample can be modelled as two layers with different rheological properties (G^*_{bulk} and $G^*_{adhesion}$) with layer heights h_{bulk} and $h_{adhesion}$ so the total gap height is $h = h_{bulk} + h_{adhesion}$. Then the apparent complex shear modulus measured by the rheometer is

$$G^*_{measured} = \frac{hG^*_{bulk}G^*_{adhesion}}{h_{bulk}G^*_{adhesion} + h_{adhesion}G^*_{bulk}} \quad (1)$$

which could be fit to a series of measurements with decreasing gaps to give G^*_{bulk} $G^*_{adhesion}$ and $h_{adhesion}$.

The effect the adhesion layer has on the measured modulus depends on both the modulus and size of the adhesion layer, which can be more clearly seen by re-writing equation (1) in a fractional form using the modulus magnitudes

$$\frac{|G|_{adhesion}}{|G|_{bulk}} = \frac{\beta}{(1-\alpha)\beta+\alpha} \qquad (2)$$

where $\alpha = h_{adhesion}/h$ and $\beta = |G|_{adhesion}/|G|_{bulk}$. For instance, if the adhesion layer is 20% stronger than the bulk modulus and the adhesion layer is 50 μm, then for measurements at 100 μm the measured modulus is increased by 9% from the bulk modulus.

This method was tested using a polymer modified binder (5%PMB130 in a 180/200 bitumen) and greywacke and stainless steel as the two aggregate surfaces. Frequency sweeps (0.1 Hz to 20 Hz) were measured at fixed %strains in the linear viscoelastic region at a variety of temperatures (5 to 45 °C) using 2.5 cm parallel plates separated by 1000 μm and then 100 μm. The modulus $|G|_{measured}$ was found to decrease as the gap decreased but the variations between the triplicate measurements were larger than any difference due to the different aggregates. Three possible explanations for this are;

- the particular aggregate/bitumen combination used doesn't form a strong adhesion layer (unfortunately time and budget constraints meant other combinations could not be tried)
- the measurements need to be made at an even smaller gap than 100 μm
- the decrease is due to the rheometer starting to measure its' own modulus rather than that of the sample. This effect occurs when the sample modulus and rheometer modulus have similar values and can be reduced by using smaller diameter plates (to increase the rheometer modulus) and/or increasing the temperature (to decrease the sample's modulus).

Other procedures used in the literature (increasing oscillatory amplitude sweeps, creep measurements, and the approach to equilibrium viscosity) were also investigated but failed to clearly differentiate between aggregates.

3. Early Adhesion Failure Due to Water Stripping

This procedure was designed to investigate early adhesion failure by injecting (distilled) water under constant pressure into the sample, to strip the binder away from the aggregate and measure this by the changing modulus using the dynamic shear rheometer. Early attempts were plagued by temperature differences between the water and binder (so changes were due to the binder changing temperature rather than being stripped).

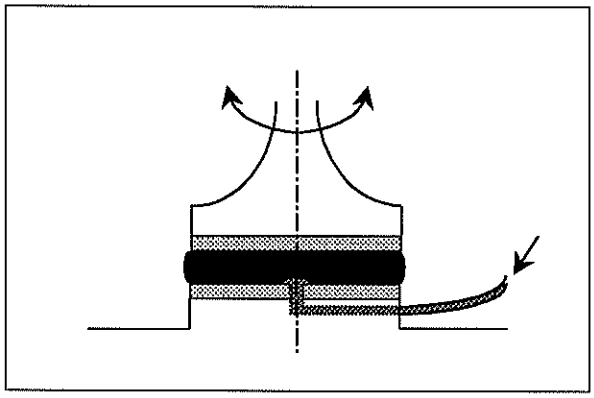

The temperature differences were removed by forming the (metal) water inlet tube into a spiral which was immersed in the same temperature control water-bath as the sample.

Using a greywacke top disk and steel bottom disk (binder = 5%PMB130 in 180/200, T= 25 °C, f = 10 Hz, and σ = 10 000 Pa), there was a slight drop in the modulus ($|G|$) when the valve was opened to allow water through, and a significant drop followed by a partial recovery when the water had tunnelled to the outside edge of the sample. Better results are seen in the phase angle, (δ), which shows significant drops (i.e. more elastic) upon opening the valve and the water reaching the sample edge. Inspection of the sample after completing the experiment suggest the water tunnelled through the bulk binder rather than stripping off the bottom plate. This implies the adhesion between the steel and binder is stronger than the binder's cohesion (at 25 °C).

Using greywacke disks for both top and bottom plates, the experiment was repeated. No changes were seen in either the modulus or phase angle although water was clearly flowing 'through' the sample. It may be that the greywacke was sufficiently porous that water escaped through the greywacke disk rather than the binder/aggregate interface or even the binder itself.

No measurement have been done with both disks being steel, and no repeat measurements were performed due to time and budget constraints. Further development of this method is needed, for instance decreasing the experiment temperature so the binder's cohesion becomes stronger then the binder/aggregate adhesion and the stripping occurs at the binder/aggregate interface (will also require increased water pressure), before it can be used to measure early adhesion failure.

4. Wetting of the Aggregate Surface

4.1 Theory

The theory for a liquid spreading on a smooth surface is reasonably well developed and is given by Cazabat and Cohen Stuart (1986, 1987) for non-volatile, completely wetting liquids spreading over a smooth, level surface as

$$A \propto V^{3/5}\left(\gamma\frac{t}{\eta}\right)^{1/5} \tag{3}$$

where capillary action is the dominant spreading force (*i.e.* for small drops), and

$$A \propto V^{3/4}\left(\frac{\rho g t}{\eta}\right)^{1/4} \tag{4}$$

where gravity is the dominant spreading force (*i.e.* for large drops). Here A is the area covered by the drop, V is the volume (which is assumed to be conserved), γ is the surface tension, η is the viscosity, ρ is the density, g is gravity and t is time the drop has been spreading. Strictly, the interfacial tension between the solid surface and the liquid ($\gamma_{ls} = \gamma_l - \gamma_s$) should be used rather than the surface tension γ_l. However the surface tension of a solid (γ_s) is difficult to measure and it is usually assumed that $\gamma_{ls} \approx \gamma_l$.

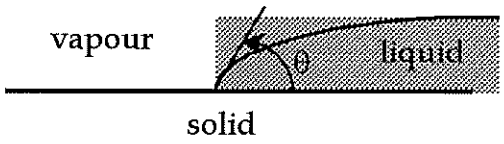

There is expected to be a transition between the capillary and gravity driven regimes at

$$R^* \approx \left(\frac{\gamma}{\rho g}\right)^{1/2} \tag{5}$$

where R^* is the radius of the (initially spherical) drop. However Cazabat and Cohen Stuart (1986) find a more complicated transition from their measurements of Silicone oil, which also depends on the spreading rate. Marmur (1983) fits a power law $A = kt^n$ to their measurements where typically $n \approx 0.20 - 0.29$ and $k \propto V^b$ with b between $0.6 - 0.72$, which shows good agreement with the theoretical exponents in equations (3) and (4).

The theory for spreading on a smooth surface depends on the edge of the liquid having the same contact angle with the solid surface around the liquid's perimeter at any one time (*i.e.* the local microscopic contact angles all equal the macroscopic contact angle). However for a rough surface no theory has been developed because the local contact angle varies around the perimeter as the liquid encounters different 'lumps' and

'troughs' in the surface (Cazabat and Cohen Stuart (1987)). Instead formulae (similar to those for spreading on a smooth surface) are empirically fit to the measurements.

Figure 1 (copied from Cazabat and Cohen Stuart (1987)) shows the various stages a liquid may pass through as it spreads on a rough surface. During the first stage the liquid forms a 'cap' which spreads as a whole. As the macroscopic 'apparent' contact angle is large, the local contact angles approximate the macroscopic angle and the liquid spreads as if on a smooth surface. Thus it may spread following $A \propto t^{1/4}$ (gravity driven) or $t^{1/5}$ (capillary driven) depending on the drop volume. In stage II the macroscopic apparent contact angle has become too small to be a good approximation to the local contact angles so a thin 'precursor' film driven by capillary forces forms in the roughness grooves ahead of the cap. The cap continues to spread at the same speed but the film expands at a rate depending on the roughness - $A \propto t^{1/2}$ for large roughness and to increasing powers as the roughness decreases. Stage III is reached when the cap has been consumed by the film, which now expands as $A \propto t^{1/2}$. Finally stage IV is when the thickness of the film becomes much smaller than the roughness and its expansion rate slows down to $A \propto t^{1/3}$.

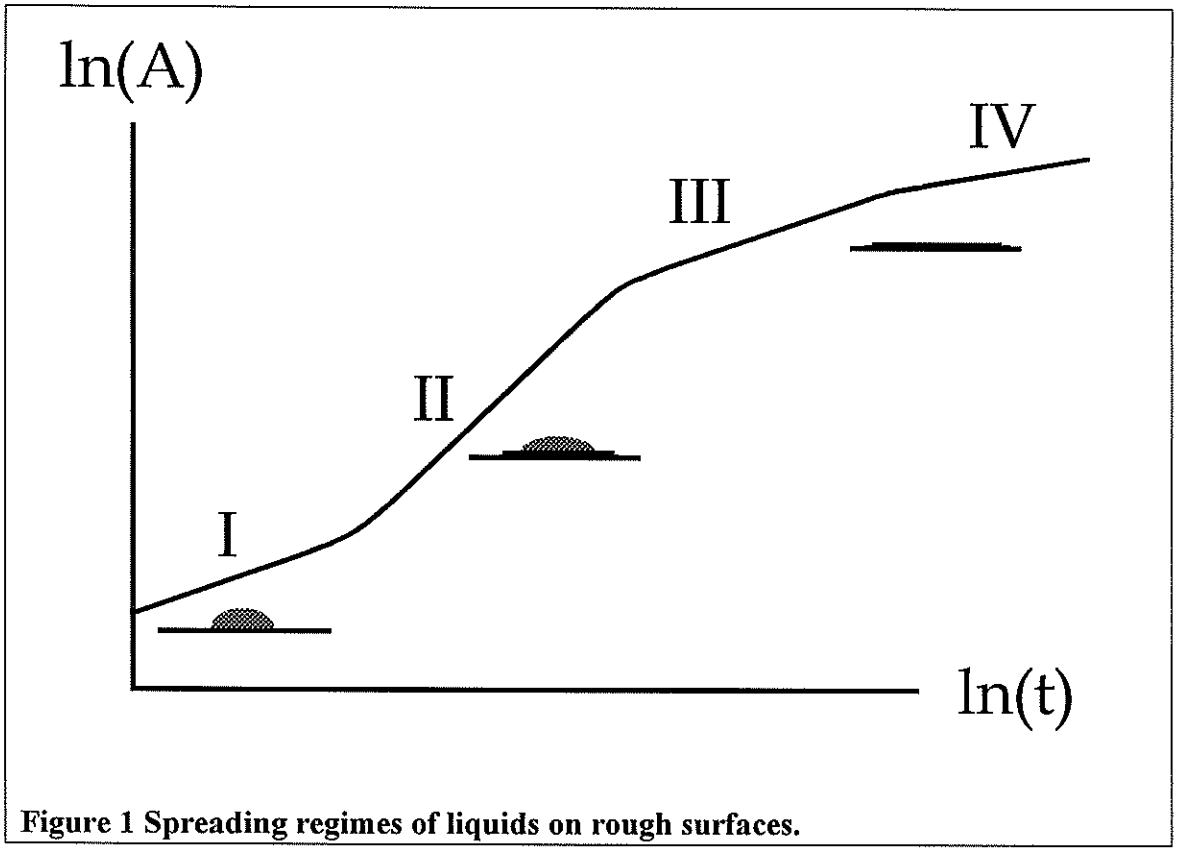

Figure 1 Spreading regimes of liquids on rough surfaces.

Apel-Paz and Marmur (1999) made measurements of liquids spreading during stages I and II and modelled the area covered by the cap as

$$\frac{A}{V^b} = k(t-\tau)^n \qquad (6)$$

by fitting k, τ, and n and assuming $b = 2/3$. The time offset (τ) reflects uncertainty in defining time zero as the measurements begin after the drop already wets the solid surface with a certain area. This can be rewritten as

$$A = k'(t-\tau)^n \tag{7}$$

by absorbing the V^b term into the new constant $k'(=kV^b)$. It is this form of the equation that will be used for the analysis in the present report (except when investigating the volume dependence – see page 24).

The precursor film was modelled by Apel-Paz and Marmur as liquid spreading into cylindrical capillaries with the capillary length taken as the difference between the radius of the film (R_{film}) and cap (R_{cap}) so

$$\frac{dR_{film}}{dt} = \frac{C}{R_{film} - R_{cap}}, \quad C = \frac{\gamma r \cos\theta}{4\eta} \tag{8}$$

where r is the capillary radius and θ is the contact angle. This requires a numerical solution, and by using the results from equation (6) for the smoothest surface and fitting C in equation (8) for the other, rougher surfaces, gave a reasonable fit to their measurements.

Apel-Paz and Marmur found that k decreased as the viscosity η increased and its dependence on the roughness decreased as the viscosity increased (presumably because the liquid had a smaller tendency to get into the roughness grooves). The power index n was independent of viscosity for smooth surfaces, but dependent for rough surfaces and sometimes showing a maximum for a certain viscosity. It also depended on the roughness but this dependence decreased as the viscosity increased.

Note that a key assumption made in the theory described above is that the values of the liquid's physical parameters (*i.e.* volume, surface tension, viscosity, density) are constant. Bituminous binders can lose weight through evaporation of more volatile components, and also gain weight through oxidation (with corresponding changes in the volume and density). However Herrington *et. al.*(1996) found a 180/200 bitumen showed less than 1% weight change (gain due to oxidation) when held at 43 °C for 3.3 years, so volume and density can be considered constant for the duration of this project's measurements. The same study found a viscosity increase of x7 after four months at 43 °C (see page 22 for discussion of possible effects on the measurements).

Recall equation (4) includes the strength of gravity (g), which is usually considered a constant. However for a chip seal there are additional forces generated by traffic acting to spread the binder which can be incorporated into a single effective force. It may be possible to simulate these forces by performing the spreading experiments in a centrifuge but that will have to wait for a future project – here it is assumed to simply scale the spreading rates in the same way for all binders.

4.2 Materials

Table 1 lists the binders used in this project, being three neat bitumen binders and two SBS PMBs at two concentrations each. The SBS binders were prepared by melting the 180/200 bitumen at 120 °C, pouring into a tin with the required amount of SBS concentrate and then heating the mixture to 160 °C and hand stirring until blended. The percentage by weight given (e.g. 3%SBS100) is that of the polymer, not the concentrate.

Table 1 Description of binders used.

Binder	Our Sample Number	Description
40/50	6/98/107	Safaniya air blown 180/200
80/100	6/97/371	Safaniya blend back 40/50 & 180/200
180/200	6/97/372	Safaniya straight run vacuum distilled
SBS100	6/98/242	20% SBS polymer concentrate (Techniflex PMB100 from Technic Industries)
SBS130	6/98/100	30% SBS polymer concentrate (Techniflex PMB130 from Technic Industries)
3%SBS100	3%SBS100	By weight 3% PMB100 polymer in 180/200
6%SBS100	6%SBS100	By weight 6% PMB100 polymer in 180/200
3%SBS130	3%SBS130	By weight 3% PMB130 polymer in 180/200
6%SBS130	6%SBS130	By weight 6% PMB130 polymer in 180/200

The moulds were made by casting Dow Corning Silastic 3481 into brass 'negative' moulds. Each sample disk was prepared by placing the required weight of binder (at room temperature) in the mould by spatula and warming in the oven until it had melted into the mould (usually 120 °C for 10 minutes). A hot air blower 'gun' was used to carefully remove any bubbles from the top surface of the sample and the sample then allowed to cool to room temperature. Sometimes upon cooling the binder shrank slightly, causing small surface dimples to appear, which could again be removed by the hot air gun. After further cooling in a refrigerator, the sample disk was be removed from the mould and replaced in reverse so the bottom surface is now on top allowing bubbles and dimples to be removed from this surface. The samples were then stored in the refrigerator (still in the moulds) until just prior to starting the experiment. Note that they should not be stored in the freezer to avoid frost or ice crystals forming on the sample.

Table 2 gives a description of the sandpaper types used in this project. The grit size reduces as the grade number increases, i.e. P60 is the coarsest sandpaper while P400 is the finest. Initially a black P400 sandpaper was used but this gave low contrast between the sandpaper and binder in the photographs so it was changed to the white version after completing the volume dependence measurements. For each experiment a circle of sandpaper (diameter ~80 mm) was glued on to a circular steel plate with Selleys general purpose multigrip. The plates are placed in trays which are adjusted to sit level while in the precision temperature oven.

Table 2 Description of sandpaper's used.

Name	Colour	Description
P60	Red	NZ Garnet paper code 02
P150	Red	Carborundum
P180	Orange	Canadian Sandpapers Ltd Gar paper AOP T0 diamond grit
P220	Orange	Canadian Sandpapers Ltd Gar paper AOP T2 diamond grit
P280	Orange	Canadian Sandpapers Ltd Gar paper AOP T2 diamond grit
P400	White	Norton NO-FIL A239 E18
P400	Black	Carborundum VO19 A965 waterproof paper

As the various grades of sandpaper used different materials for the grit, glue and paper backing, the grades will have different surface tensions in addition to the grit size and spacing. Thus the sandpaper 'texture' will have to be treated as categorical variable during any analysis, rather than the numeric variable implied by the grade number.

4.3 Measuring Procedures

The diameters were measured in two ways; first 'by eye' holding a ruler just above the samples, and secondly off photographs taken of the samples. It was hoped that the 'by eye' method would give sufficient accuracy and precision to be used for all future measurements, as it is both quicker and cheaper than the photographic method. However it was found to over-estimate the diameters (due to parallax errors), and also become less accurate as the samples spread across the sandpaper losing their initial circular outline.

The photographic method used a Pentax camera with a close-up ring between the camera body and lens. Desk-lamps illuminated the sample from all sides to reduce the effect of variations in natural lighting and remove shadows cast by the top edges of the sample. The photograph prints were photocopied to a larger size (typically 3x) and the sample area in the photocopy measured by a digital planimeter. A ruler was included in the photographs to provide the scale.

A typical photograph is shown in Figure 2. The number (91) identifies particular the bitumen type/mass/diameter, sandpaper and oven temperature combination, while the time in the oven is indicated by the stop watch (72 hours). The main disk of the sample is still spreading in a smooth, nearly circular shape. This sample also shows the precursor thin film discussed earlier (see page 16), which is now spreading in a irregular (fractal) pattern ahead of the main disk. However this sample was atypical in that there is a large separation between the precursor and bulk disk which is also clearly visible in the photograph. In the majority of samples it was often impossible to separate the main disk from the precursor film from the photographs so all planimeter measurements were around the outermost edge of the sample (regardless of whether it was the main disk or a precursor film). Therefore investigating the different behaviours of the main disk and precursor film will have to be left to a future project.

A typical set of measurements is shown in Figure 3, together with the non-linear least squares fitted curve based on equation (12). The time offset (τ) here also includes the effects of the binder warming to the oven's temperature, and the initial cylindrical shape of the binder 'disk' changing to a hemispherical 'cap' shape in addition to the area already covered by the disk at the beginning of the experiment.

Figure 2 Photograph of typical sample binder spreading on sandpaper.

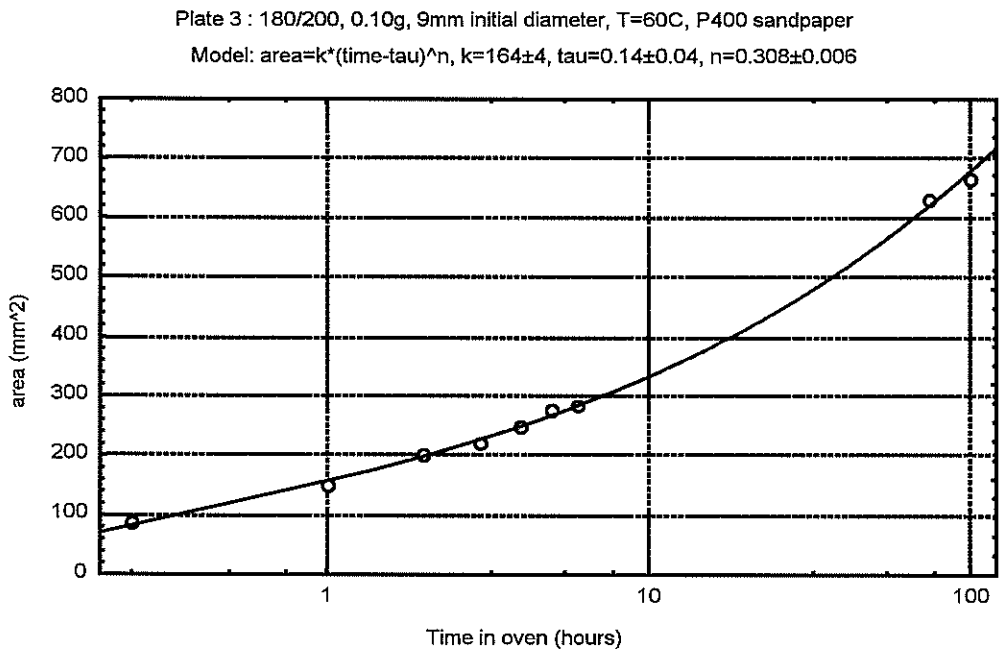

Figure 3 A typical growth curve for a binder spreading on sandpaper.

To check for errors in measuring the area of the binders, a circle of graph paper ruled with a 1 mm grid was glued on a steel plate in place of a sandpaper / binder combination. A series of rectangles with different areas were marked on the graph paper and measured with the planimeter from the enlarged photocopy of the photograph. The results of these measurements are graphed in Figure 4. The systematic errors are indicated by the fitted curve with a linear term due to a small error (~0.5%) in scaling the planimeter raw measurements to square millimetres and possibly a sinusoidal term (±2.4 mm²). If this oscillatory error is real, it could be due to an optical distortion in either the camera, photograph processing or photocopying. Except for the measurements of the two smallest rectangles, the random errors all have a standard deviation of about 0.5%. After allowing for operator variability in using the planimeter and that the binder outlines will harder to measure than simple rectangles, a 1% standard deviation seems a reasonable estimate of the random errors.

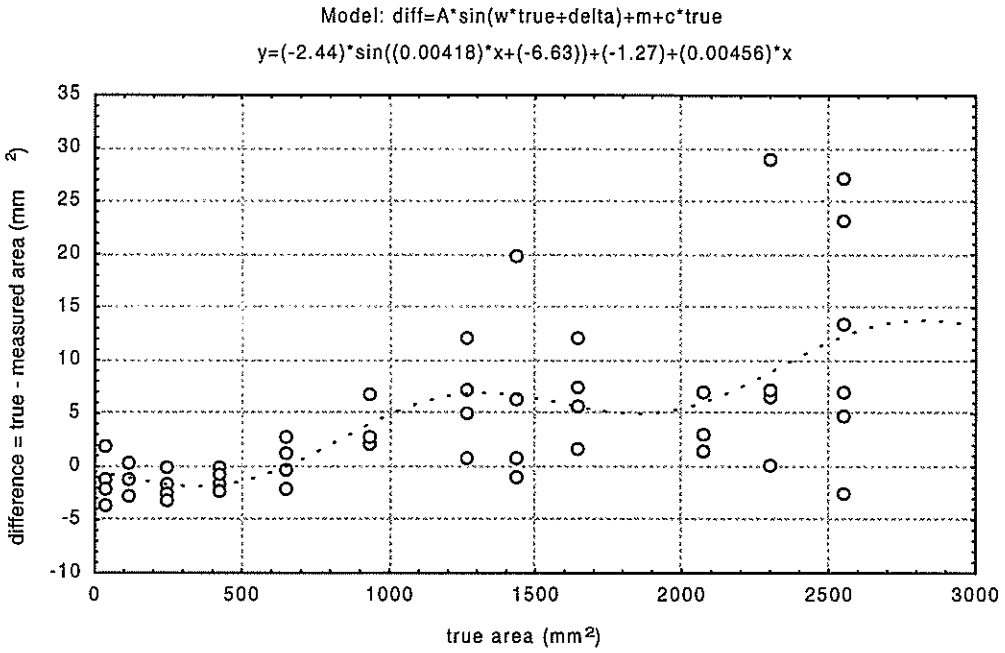

Figure 4 Errors in the procedure for measuring the area.

The actual measurements may also be used to look for this possible sinusoidal error, as shown in Figure 5. The solid curve in the top graph is the normal fit (using equation (7)) while the bottom graph shows the residuals between the expected and measured areas. These residuals give good agreement with a sinusoidal term but have a significantly larger amplitude (51 mm^2 compared with 2.4 mm^2) than in Figure 4. This large amplitude means the residuals are probably not due to the possible optical distortion discussed earlier. It should also be noted that this oscillatory residual is not found in all samples (e.g. see Figure 3).

An alternative explanation for these residuals could be oscillations in the binder (with the elasticity of the binder trying to retain its prior shape in opposition to the spreading forces), with the period of oscillation related to the area of the binder and so continuously increasing. This can be simultaneously fit with the growth curve using

$$\begin{aligned} y &= k'(t-\tau)^n \\ \text{area} &= y + A\sin(\omega \cdot y + \delta) \end{aligned} \tag{9}$$

which now has 6 free parameters. To get a well conditioned fit requires at least 12 data points appropriately spaced over a complete sinusoidal cycle (compared with the originally planned 6 points minimum required for fitting equation (7)). The dashed curve in the top graph shows the results adding the (separately fitted) growth curve and residuals together

A third possibility could be changes in the binder viscosity, for example due to steric hardening. This could be modelled as an exponential growth to a final viscosity

$$\eta = \eta_0 + \Delta\eta(1 - e^{-t/\tau_\eta}) \tag{10}$$

and the area growth curve now becoming

$$A = k''\left(\frac{t-\tau}{\eta}\right)^{n} \tag{11}$$

which now has six free parameters. Again insufficient data points were measured to fit these equations but calculations using plausible viscosity values (taken from Herrington *et. al.*(1996)) generate growth curves similar to those measured. Compared to growth curves where the viscosity remains unchanged from its initial value η_0, k'' and τ are increased while the power index n is decreased.

As investigating the cause of these residuals is beyond the scope of this project, it was decided to remain with fitting equation (7) and treat the residuals as an additional random error.

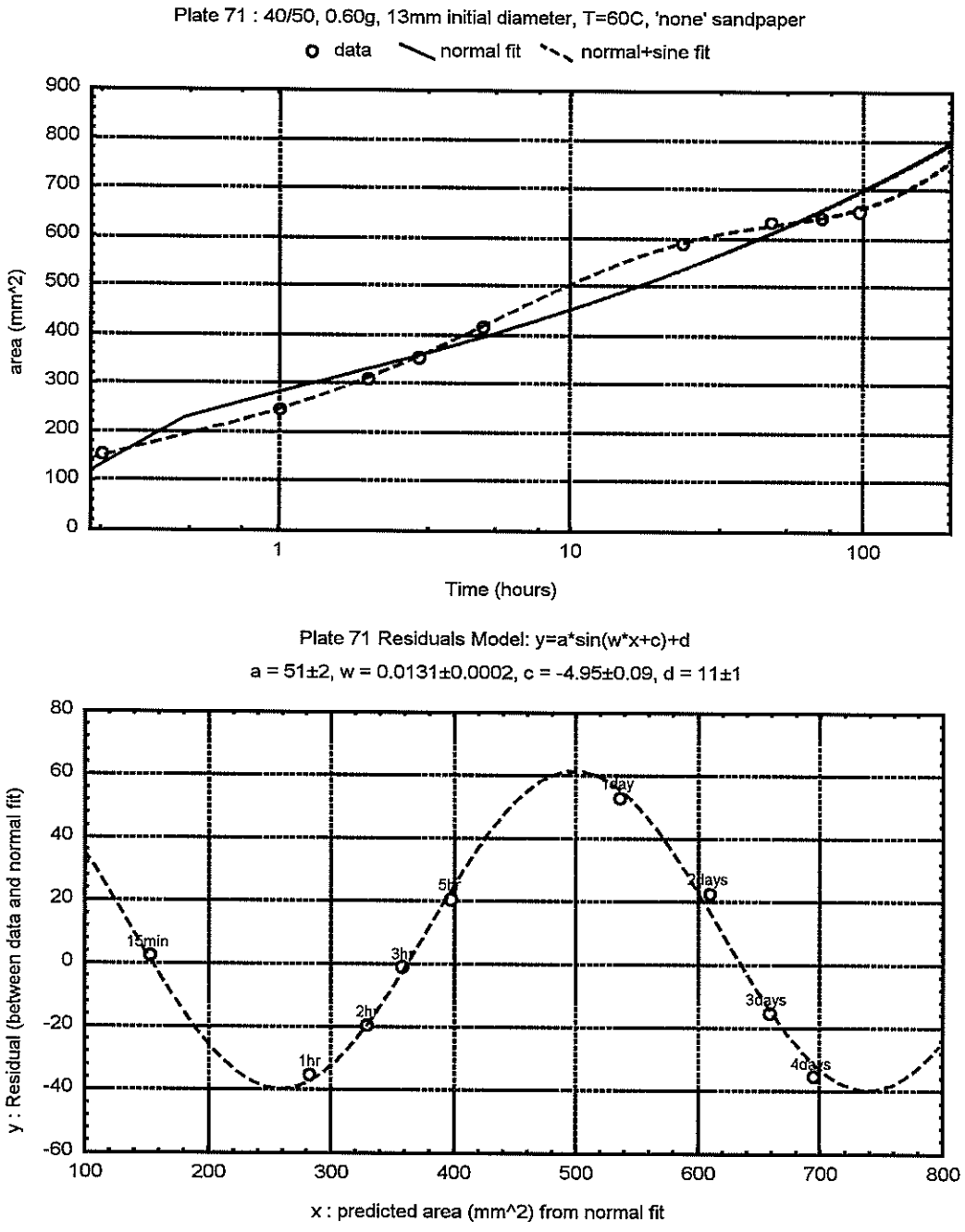

Figure 5 Residuals from measuring the growth curve for a binder spreading on sandpaper.

4.4 Volume Dependence

Recall that equation (6) states the rate at which the sample spreads depends on its volume V (raised to some power b). This can be rearranged to

$$A = k'(t-\tau)^n, \quad k' = k\left(\frac{m}{\rho}\right)^b \tag{12}$$

where m is the sample mass, and ρ is the density (which is constant for a particular bitumen / temperature combination) as $\rho = m/V$. Taking natural logarithms of k' gives

$$\ln(k') = \{\ln(k) - b\ln(\rho)\} + b\ln(m) \qquad (13)$$

which is a straight line with slope b.

To investigate if this holds for PMBs, sample disks of the neat 180/200 bitumen and the 6%SBS130 PMB were prepared in the mass/initial diameter combinations listed in Table 3. Duplicate samples of the same combination are indicated by double ticks. The samples were placed on P400 grade sandpaper and their average diameters measured at various intervals after placing in a precision oven set to 60 °C.

Table 3 Sample diameters and masses used to investigate spreading dependence on volume.

All samples either 180/200 or 6%SBS130 binder measured at 60 °C on P400 sandpaper											
Diameter (mm)	**Mass (g) {proportional to volume}**										
	0.10	**0.15**	**0.20**	**0.25**	**0.30**	**0.40**	**0.50**	**0.60**	**0.75**	**1.00**	**1.25**
9.0	√	√√	√	√√	√						
13.0		√√		√√		√	√√	√			
18.0				√√			√√		√	√	√

The result of fitting equation (12) to each sample / sandpaper combination in Table 3 is shown in Figure 6 and Figure 7. There are clear differences in the fitted parameters between the two binders, with the 180/200 binder generally having a larger value of k' but smaller n for any particular mass. Although larger values of either k' and n mean a faster spreading rate, inspection of graphs such as Figure 3 show k' has a greater effect than n for the values encountered in this project.

There is a clear change in the spreading rate parameter k' with the mass (or equivalently the volume) of the samples, with the volume being raised to the power of $b = 0.82 \pm 0.03$ for the 180/200 bitumen and $b = 0.73 \pm 0.11$ in the 6%SBS130 PMB. As the two values overlap (given the size of the standard errors), there is no significant difference in the volume exponent b between the two binders. The weighted mean is $b = 0.80$, which is only slightly higher than the theoretically expected value (0.75, see equation (4)) for *liquids* spreading by gravity on *smooth* surfaces. The dashed curves in Figure 6 indicate the 99% confidence limits about the linear least squares fits.

There is a clear dependence on the sample volume for the time exponent n, as shown in Figure 7 with the curves in the figure drawn solely to guide the eye. As the surface tension of a typical bitumen is 30×10^{-5} N/cm (from Hoiberg (1964)) and density 1.0 g/cm^3 (The Shell Bitumen Handbook (1990)), then equation (5) predicts the transition between capillary and gravity spreading will occur for a drop of mass ~0.03 g. Thus it is likely the change in n at the smaller masses is part of a transition region between capillary and gravity driven spreading even though the actual values of n are somewhat

larger than those predicted by equation (4). However further investigation will have to await a future project.

As n becomes independent of volume for masses greater than ~0.50 g, all samples used in the rest of this project were cast as 0.60 g disks with an initial diameter of 13 mm.

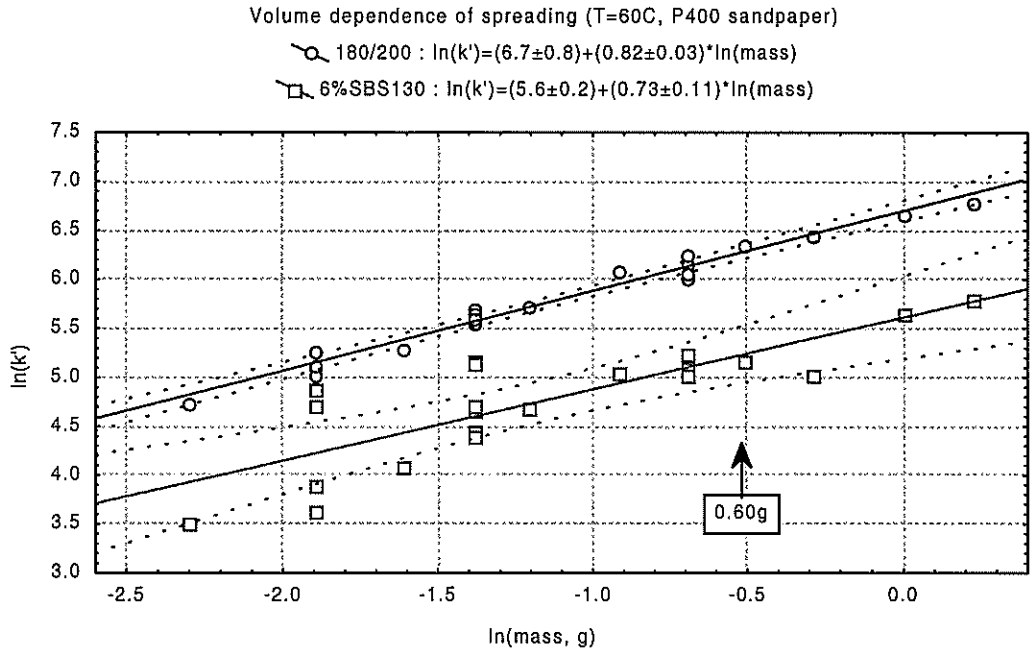

Figure 6 Effect of sample volume on binders spreading parameter k'.

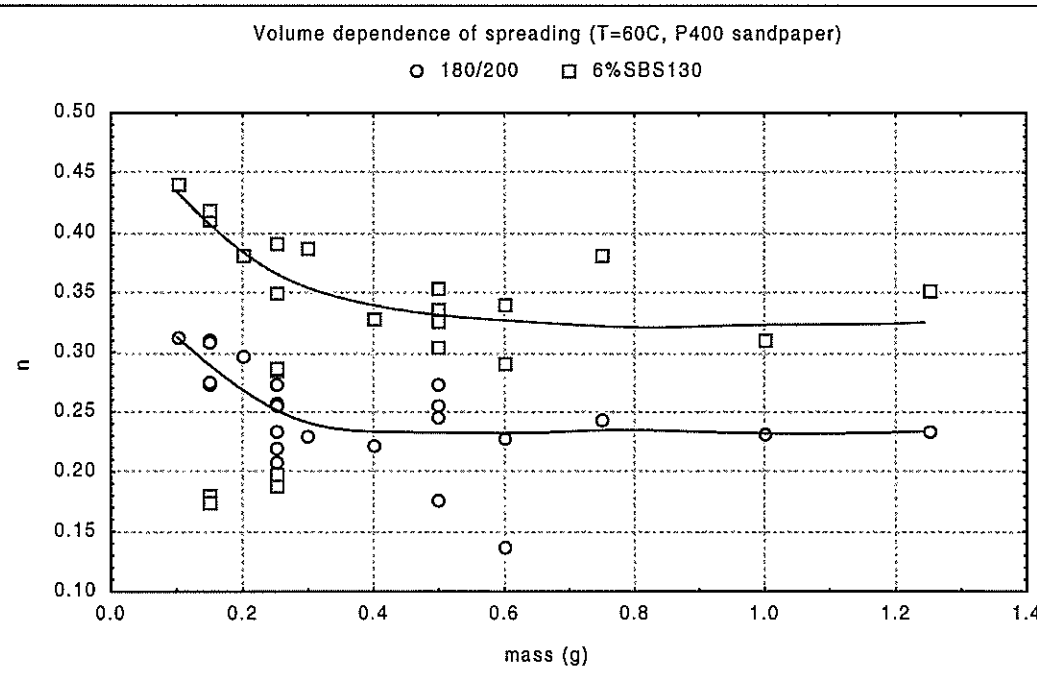

Figure 7 Effect of sample volume on binders spreading parameter n.

4.5 Texture Dependence

To investigate if the spreading rate depends on the texture (roughness) of the surface, the binder / sandpaper combinations listed in Table 4 were measured at 60 °C for 0.60 g disks with initial diameters of 13 mm. One texture, labelled 'none', is achieved by placing the sample disk directly on the steel backing plate rather than on sandpaper. This provides the smoothest surface used in the project.

Table 4 Binder / sandpaper combinations used to investigate spreading dependence on texture.

Texture (sandpaper)	Binder (all at 60 °C and mass = 0.60 g with an initial diameter 13 mm)						
	180/ 200	80/ 100	40/ 50	3% SBS130	6% SBS130	3% SBS100	6% SBS100
P60	√√	√√	√√	√√	√√	√√	√√
P150	√		√		√		√
P180	√√	√√	√√	√√	√√	√√	√√
P220	√		√		√		√
P280	√		√		√		√
P400	Already done	√√	√√	√√	Already done	√√	√√
none	√	√	√	√	√	√	√

An Analysis of Variance (ANOVA) test was used to see if the spreading rate depends on the surface texture, with the results shown in Table 5. To allow comparisons with results obtained earlier (while investigating the volume dependency) the spreading parameter k' will continue to be used rather than k. Each spreading rate parameter (k' and n) was tested separately, and in combination, for each binder. A large F-statistic indicates the texture does affect the relevant spreading parameter, as does a small confidence level (p-level). For the analysis of the k' and n together, the Raos R statistic approximates the F-statistic. As a quick guide, the ticks in the 'p<5%' columns indicate if the parameter can be considered to be affected by the texture with greater than 95% confidence.

Table 5 ANOVA results of spreading rate dependence on texture.

Binder	Dependent variable = k'			Dependent variable = n			Dependent variables = k' and n		
	F	p-level	p<5%	F	p-level	p<5%	Raos R	p-level	p<5%
180/200	1.03	0.53		15.8	0.02	√	14.2	0.01	√
80/100	8.3	0.06		36.9	0.006	√	11.8	0.02	√
40/50	9.2	0.05	√	5.2	0.10		2.0	0.26	
3%SBS130	2.4	0.24		24.6	0.01	√	5.0	0.07	
6%SBS130	3.0	0.20		3.6	0.16		2.7	0.18	
3%SBS100	7.9	0.06		38.3	0.006	√	11.3	0.02	√
6%SBS100	7.7	0.06		24.6	0.01	√	15.6	0.01	√

The k' parameter is largely unaffected by the texture, with only one binder (40/50) being significantly affected at the 5% level. However four binders are affected if the confidence level is relaxed to 90% (p<10%). The n parameter is strongly affected by texture, with the only binders not affected (40/50 and 6%SBS130) being those with the largest viscosity which agrees with Apel-Paz and Marmur (1999). This also holds for

the overall spreading rate (k' and n together), with only the lower viscosity binders being affected by texture. From inspection of the parameter values, there may be a tendency for n, and hence the spreading rate, to increase as the sandpaper texture becomes coarser.

However it is possible that larger viscosity binders not being affected by the texture level is an experimental artefact. This is because the measurements were all stopped after the same time interval in the oven (96 hours) rather than after each sample had spread out to the same final diameter. If the effect of texture on the spreading rate does not become apparent until the sample has spread out to a sufficiently large diameter, then it won't have been detected in the higher viscosity binders. Further work on this, and untangling the effect of grit size and differing surface tensions from different sandpaper materials (which was lumped together as a 'texture' category here), will need to be addressed in a future project.

4.6 Temperature Dependence

The binder and sandpaper combinations used to investigate the effect temperature has on spreading rates are listed in Table 6. Originally measurements were also planned for 25 °C and 50 °C . However the precision temperature oven was found to be unstable at 25 °C (it was too close to the ambient temperature) so the measurements had to be abandoned at that temperature. Extra measurements were carried out at 30 and 40 °C so the 50 °C measurements were not required.

Table 6 Binder / sandpaper combinations used to investigate spreading dependence on temperature.

Temperature (°C)	Binder (on P60, P280 & 'none' textures and mass=0.60 g, with an initial diameter 13 mm)						
	180/ 200	80/ 100	40/ 50	3% SBS130	6% SBS130	3% SBS100	6% SBS100
30	√√	√√	√√	√√	√√	√√	√√
40	√	√	√	√	√	√	√
60	Already done	Already done	Already done	Already done	Already done	Already done	Already done

The results are summarised in Figure 8, where data points with large values of k' and n indicate a binder that rapidly spreads across the sandpaper. All textures are included in the plot as we want binders that will spread well across an aggregate surface regardless of its particular texture. Two curves, $k' \cdot n = 27$ and $k' \cdot n = 44.5$, divide up the plot into regions of poor, marginal and good binders when measured at 40 °C. At the moment these curves are somewhat arbitrary, being based on;

- At T=60 °C, all binders should show good wetting and spreading rates
- At T=40 °C, expect to have binders in all three regions (of good, poor and marginal)
- At T=30 °C, only the best binders should show marginal spreading rate

This temperature (40 °C) was chosen as the results show good discrimination between the different regions and take an acceptable period to measure (approximately a week).

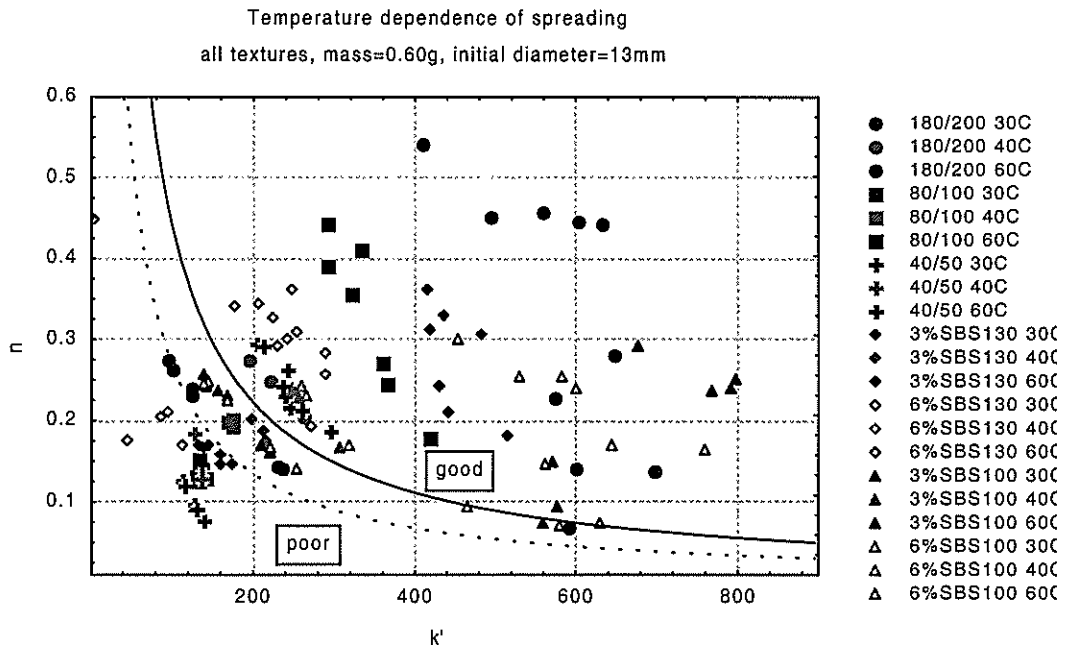

Figure 8 Curve fitting parameters for good verses poor spreading rates.

Based on these curves and the 40 °C results, the 180/200, 3%SBS100 and 6%SBS100 would be considered to show good wetting, the 80/100 and 3%SBS130 marginal wetting and the 40/50 and 6%SBS130 unacceptable wetting.

An alternate way to look at the same data is to plot the time taken by each binder to cover a particular area, based on equation (7) and the fitted parameters k' and n. This area (~400 mm²) was chosen to be three times the original area, which for a hypothetical binder corresponding to a 'good' binder ($k' \cdot n = 27$ in Figure 8) took 24 hours. The time is then normalised by dividing by 24 hours, so a time less than 1 indicates a 'good' binder. For clarity, the data is only plotted for two sandpaper textures; the coarsest texture (P60, see Figure 9) and the smoothest texture (on the stainless steel plate, see Figure 10). The graphs show how sensitive the spreading rates are to temperature, for instance the 3%SBS130 binder takes 10 times longer to wet the aggregate for a 10 °C temperature decrease from 40 °C to 30 °C.

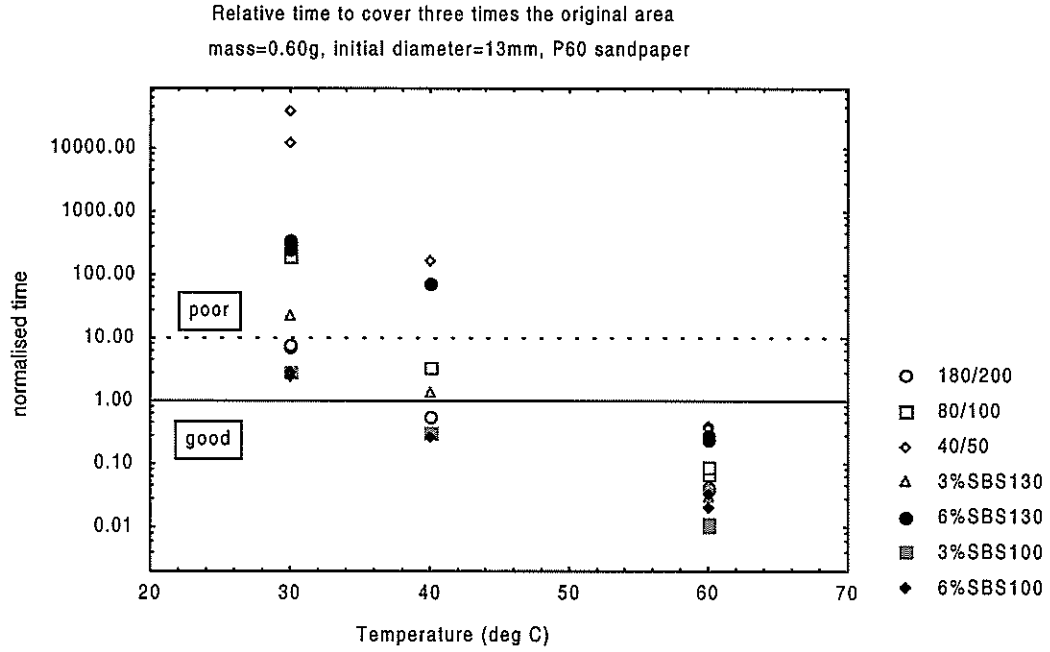

Figure 9 Predicted time to triple the area covered on P60 sandpaper.

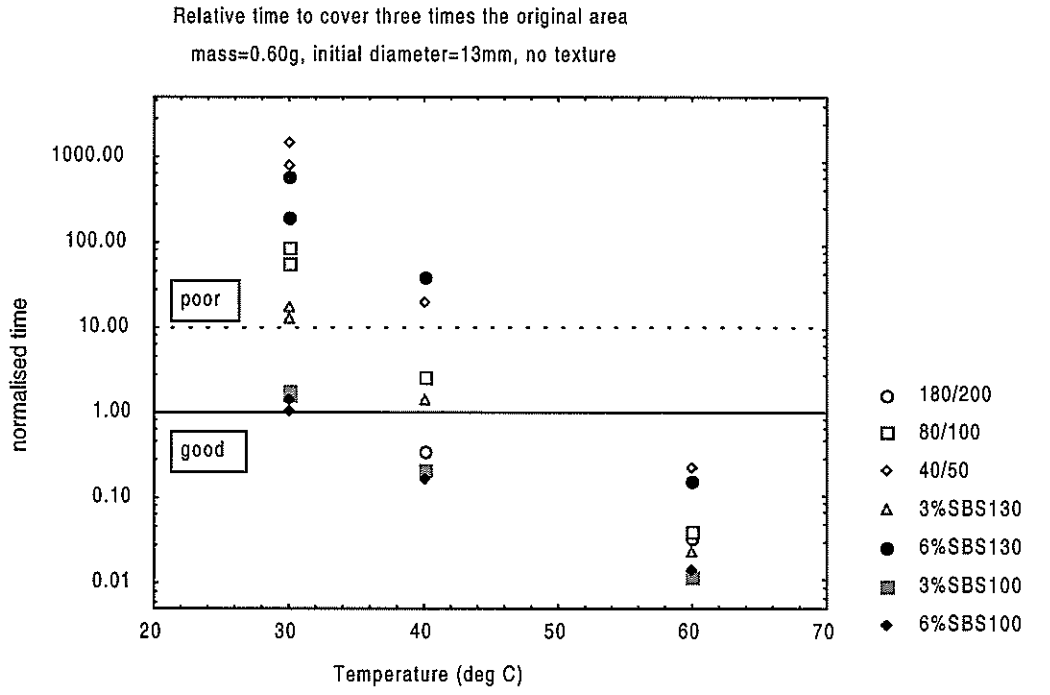

Figure 10 Predicted time to triple the area covered on smooth texture.

5. Conclusions

It was expected that a binder's modulus would increase as the film thickness decreased, due to measurement of an adhesion layer between the binder and aggregate surfaces. However, in the particular combinations of binder and aggregate tested here, the modulus decreased in a manner apparently independent of the type of aggregate. This is probably due to the high value of the sample modulus so the rheometer starting to measure its own (lower) modulus as the sample thickness decreased, and would need to be remedied by using smaller diameter rheometer plates (to increase the rheometer modulus) and/or measuring at higher temperatures (to decrease the binder's modulus). However at this time the existence of a higher modulus layer forming due to adhesion between the aggregate and binder can not be confirmed.

Water (under constant pressure) was found to flow through a PMB bonded to a stainless steel surface at 25 °C, and produce significant changes in the modulus as it did so. However, it was found that the water tunnelled through the middle of the sample rather than stripping the binder away from the aggregate. This implies the adhesion between the binder and steel 'aggregate' was stronger than the binders cohesion. With a greywacke surface, no change in the rheology was found even though water was clearly flowing so it appears the water was flowing through the greywacke itself rather than the binder.

A simple growth (power) law was found to give a good first order approximation to the measured spreading rate of binders on rough surfaces. However some (second order) discrepancies were found, possibly due to elastic oscillations or steric hardening of the binder, which need further investigation. The spreading rates were found to depend on the surface's roughness, especially for lower viscosity binders. However the largest influence on the spreading rates is temperature, for instance a 3%SBS130 binder takes ten times longer to cover the same area when the temperature drops from 40 °C to 30 °C. Measurements at 40 °C were found to give good discrimination between binders with acceptable/unacceptable spreading rates, but this finding needs to be calibrated against field results before the method could be put forward for consideration as a standard test.

6. Recommendations for Future Research

During this project several questions arose which could not be answered because they were either outside of the scope of this project or due to time and budget constraints. These are recommended for future research, and are listed below;

- Different aggregate/binder combinations (together with different measuring conditions such as thinner binder layers and smaller diameter rheometer plates) be investigated for the formation of an adhesion layer between the binder and aggregate.
- The areas covered by the precursor film and the bulk of a binder spreading over the (sandpaper) 'aggregate' surface should be measured separately.
- Further investigation into the cause (measuring distortions, elastic oscillations, steric hardening?) of the sinusoidal residual from the power growth law (which describes the spreading rate of the binder over the aggregate surface) is needed.
- The transition between capillary and gravity driven spreading should be measured using smaller drop sizes of the binder.
- The validity of using sandpaper as a model aggregate needs to be investigated, together with the measurement reproducibility, ease of preparation and expense of using real aggregate surfaces.
- The degree to which a binder's spreading properties can be explained by its rheological properties (elastic and viscous modulus) needs investigation.
- A larger variety of PMBs need to be measured.

7. References

Apel-Paz, M. and Marmur, A. 1999. Spreading of liquids on rough surfaces. *Colloids and Surfaces A: Physicochemical and Engineering Aspects, 146:* 273-279.

Bikerman J. J. 1966. *Journal of Materials 1:*34.

Cazabat, A. M. and Cohen Stuart, M. A. 1986. Dynamics of Wetting : Effects of Surface Roughness. *J. Phys. Chem., 90:* 5845-5849.

Cazabat, A. M. and Cohen Stuart, M. A. 1987. Dynamics of wetting on smooth and rough surfaces. *Progress in Colloid & Polymer Science, 74:* 69-75.

Ensley E. K. 1975. *Journal of Applied Chemical Biotechnology 25:* 67.

Ensley E. K. and Scholz H. A. 1972. *Journal of the Institute for Petroleum 58:* 95.

Fink D. F. and Griffin R. L. 1961. Measurement of the consistency of paving cements at 140F with the sliding plate microviscometer. *American Society for Testing Materials, Special Technical Publication No. 309:* 79-93.

Gastmans A. C. 1996. Asphalt rheology on thin film. *Petersen Asphalt Research Conference, 33rd Annual Meeting,* July 15-17, Laramie, Wyoming.

Herrington, P. R. Patrick, J. E. Hamilton, P. G. and Forbes, M. C. 1996. Non-volatile flux for chipsealing : Laboratory study interim report. *Transfund New Zealand Research Report 71.*

Hoiberg, A. J. (ed.) 1964. *Bituminous Materials : Asphalts, Tars, and Pitches.* Volume 1, Wiley & Sons.

Huang S-C, Robertson R. E., McKay J. F., and Branthaver J. F. 1998. A study of low temperature hardening of thin film asphalt binder in contact with aggregate surface. *Petroleum Science and Technology, 16(7&8):* 869-902.

Mack C. 1957. *Industrial and Engineering Chemistry, 49:* 422-427.

Marmur, A. 1983. Equilibrium and spreading of liquids on solid surfaces. *Advances in Colloid and Interface Science, 19:* 75-102.

Scholz T. V. and Brown S. F. 1996. Rheological characteristics of bitumen in contact with mineral aggregate. *Journal of the Association of Asphalt Paving Technologists 65:* 357-384.

Shell Bitumen UK 1990. *The Shell Bitumen Handbook.*